Impact of ion irradiation on the thermal, structural, and mechanical properties of metallic glasses

S. G. Mayr*
I. Physikalisches Institut, Georg-August-Universität Göttingen, Friedrich-Hund-Platz 1, 37077 Göttingen, Germany
(Received 14 September 2004; revised manuscript received 22 November 2004; published 18 April 2005)

The impact of ion-beam irradiation on the thermal, structural, and mechanical properties of metallic glasses is investigated using the model glass, CuTi, in molecular dynamics computer simulations. It is found that ion-beam bombardment successively modifies the compositional and structural order toward a universal steady state, which proves to be independent of the initial relaxation state and thermal history of the unirradiated sample. This is reflected by key materials properties, including enthalpy, structural and compositional short-range order, as well as Young's modulus and fracture behavior. The results are interpreted within the framework of competing dynamics, where radiation-induced plastic relaxation counteracts ion-beam disordering.

DOI: 10.1103/PhysRevB.71.144109 PACS number(s): 61.43.Dq, 61.80.Jh, 61.82.Bg

I. INTRODUCTION

For more than 50 years[1,2] ion-beam interaction with matter has attracted high scientific interest, where the main focus was lying on defect generation, modification of mostly crystalline metals and semiconductors, as well as ion implantation. Despite this rather long history, ion beams continue to be an exciting tool, especially for applications with new materials and nanoscale-structured matter (see Ref. 3 for an overview). Within this scope, ion beams basically constitute a tool for locally generating a thermodynamic activation, which is capable of materials modification, and subsequently relaxes back toward a local, often metastable, equilibrium.[4] This idea is being extensively studied within the framework of driven systems.[5]

The present work investigates a related topic, viz. ion-induced modifications of the thermodynamic, structural, and mechanical properties of metallic glasses from an atomistic point of view, using molecular dynamics (MD) computer simulations. Since the development of new glass-forming alloys, metallic glasses have become increasingly popular during the last decade—from a scientifically fundamental point of view and also as engineering material.[6] When an ion beam hits a glassy metallic solid, the ion-solid interaction in the early stages of the collision cascade is comparable to its crystalline counterpart. However, because of the random nature of glassy matrix and the absence of lattice constraints, activated entities in the glassy solid, such as defects or molten zones, are expected to rearrange pretty freely during relaxation or resolidification, respectively. If stresses are applied, these effects can lead to plastic deformation,[7–9] which can be utilized for surface smoothening[10] or stress modification[11] in amorphous thin films. Internal structural relaxation in metallic glasses because of thermodynamic driving forces is expected to be closely related to plastic relaxation under external forcing, in the case of annealing treatment, as well as ion bombardment. In fact, for the thermal case, an internal viscosity can be successfully introduced, which governs structural relaxation, in close relation to the shear viscosity.[12] Under ion bombardment similar effects are expected. They are, however, experimentally hardly accessible because of the impossibility to atomically resolve modifications in the glassy matrix. Resistivity measurements during ion-beam bombardment of metallic glasses indicate severe structural modifications.[8] However, it seems greatly impossible to map resistivity changes to structural rearrangements or defects because of the complexity of the phenomena. In a simulation work, Mattila *et al.*[13] addressed a related issue by considering a single irradiation event in an icosahedrally ordering system, where the order was initially destroyed and subsequently partly restored within the course of a single thermal spike.

We employ MD computer simulations[14] using realistic interatomic potentials for the model glass, CuTi,[15] to bring more light into this exciting issues of radiation-induced structural modifications. It is expected that such simulations are highly realistic, as they have proven to model radiation-induced materials processes in crystalline and amorphous metals even quantitatively correct.[9,11,16,17] One of the main underlying reasons is the possibility to fully cover the time scale of a collision cascade in MD simulations, if low enough base temperatures of the simulation cell are chosen. This is in complete contrast to thermally activated relaxation processes in glasses, which require extraordinary long simulation runs to cover all relevant materials processes and are consequently performed in very small simulation cells.[18].

The paper is organized as follows: After reviewing the details of the simulation procedures in Sec. II, thermodynamic aspects are treated in Sec. III, followed by radiation-induced structural modifications (Sec. IV) and the investigation of the mechanical properties (Sec. V). Finally, the results are discussed in a broader context in Sec. VI, followed by the conclusion and an outlook.

II. SIMULATION METHODS

MD simulations[19] are performed using the interatomic embedded atom method[20] (EAM) potentials, as parametrized by Sabochick and Lam.[15] The long-range cutoffs were chosen as described in the original publication, while the short-range pair interactions were splined to Ziegler-Biersack-Littmark universal potentials;[21] the corresponding electron

densities were smoothly joined away using third-degree polynomials, as described before.[22]

Glassy simulation cells are prepared by quenching from melt at variable rates and zero pressure. Additionally, for comparison, a most completely relaxed reference cell is obtained by successive heating and quenching cycles. During these quench runs, the temperatures and pressures of all atoms are controlled via Berendsen[23] temperature and pressure controls, respectively. Ion irradiation is simulated by successively assigning randomly directed velocities of the specified kinetic energy to randomly selected recoil atoms of random type, while periodic boundary conditions are maintained in all spatial directions. This approach guarantees a homogeneous damage distribution throughout the whole cell at high enough doses, while primary ions (originating from outside the sample) and all effects related to them, other than causing a collision cascade, are omitted. This allows us to focus solely on radiation-induced structural changes introduced by energetic impacts, excluding surface and impurity effects. Although this is surely an idealized situation, it can experimentally occur in that portion of volume that is located far enough apart from the open surface and the implantation depth of the primary ions, respectively (e.g., inside a thin films, where the primary ions are implanted into the substrate). The number of atoms in the simulation cell was scaled with the maximum recoil energy to prevent any considerable heating of large fractions of the cell. As rule of thumb it was assured that more than 35 atoms were present per recoil-introduced electron volt. During simulated ion irradiation, only the outermost two rows of atoms of the cells were damped to the desired temperature, using, again, a Berendsen temperature control. It was, however, assured that neither any recoil nor energetic atom from within the collision cascade reached the thermostated regions. This procedure thus simulates the heat flow from the cell into an infinite surrounding crystal. The strength of the temperature coupling was chosen to maximize energy absorption and minimize shock-wave reflections/transmissions at the boundaries.[24] Electronic stopping was incorporated as a frictional force, which affects all atoms with a kinetic energy exceeding 10 eV; it was based on the SRIM[25] stopping powers. During the lifetime of each individual recoil cascade, the cell boundaries were fixed to prevent artifacts caused by an oscillatory response of the pressure control. This approach slightly overestimates the pressure during a volume cascade in comparison to the experimental situation, where the surrounding lattice may elastically yield. However, test runs on individual recoils, which were performed at various hydrostatic pressures (−4, 0, and 4 GPa) and cell sizes, did not show any influence on the properties investigated within the current scope.[26] Before starting a succeeding recoil, the pressure is optionally equilibriated toward zero—the omission or insertion of this step enables us to simulate isochoric and isobaric conditions, respectively. However, for metallic systems, the results proved to be identical. In analogy to crystalline samples, the damage is characterized by the displacements per atom (dpa), which are determined from the Kinchin-Pease[27] expression, using the displacement energy 10 eV, as determined before.[9] The amorphous nature is verified by calculating the radial and angular distribution functions, as well as by monitoring the presence of a glass transition in the enthalpy and volume during quenching and successive annealing. In the present study, amorphicity was maintained independent of the treatment. Generally, the structural information that is provided by the radial distribution function (RDF) is rather limited. Depending on the requirements, therefore, various differently sophisticated methods have been proposed to decompose the first coordination shell to obtain additional information.[28–31] In the present work, the main interest lies on the comparison of the amorphous short-range order (SRO) with specific energetically favored crystalline (fcc, hcp, bcc) or icosahedral (ico) configurations. Therefore, the structural order parameter P_{st}, as introduced by Zhu *et al.*,[31] is employed

$$P_{st}(k) = \sqrt{\frac{\sum_i [\theta_k(i) - \theta_k^p(i)]^2}{\sum_i [\theta_k^\mu(i) - \theta_k^p(i)]^2}}. \quad (1)$$

Here, $\theta_k(i)$ denotes the ith smallest angle formed with atom k at the vertex and its two neighbor atoms, θ_k^p is the same quantity for the perfect lattice, and $\theta_k^\mu(i) = [2\pi i / n_{nb}(n_{nb}-1)]$ is the uniform angular distribution (n_{nb} is the number of nearest neighbors). Systematic tests showed that although the values of P_{st} for fcc, hcp, bcc, and ico shells are to some degree coupled, it is clearly possible to discriminate them by introducing an appropriate cutoff, chosen as 0.25: If $P_{st} < 0.25$ for a specific coordination shell, then it is defined to have an order as specified by θ_k^p.

Additionally, compositional changes in the nearest-neighbor shell are monitored by calculating its average composition in dependence of the type of the central atom, Cu or Ti.

To determine specific physical properties, such as the Young's modulus E or the fracture behavior, more simulation runs are performed with appropriate boundary conditions, as well as temperature and pressure controls enabled. To determine E, the cell is loaded with 0.1 GPa and zero stress, respectively, using a Berendsen pressure control with periodic boundaries employed.[32] To determine the fracture behavior, stress-strain curves with open boundaries in x/y and periodic boundaries in the z direction are utilized, using the strain rate, $\dot{\epsilon}_{zz} = 5\ \mathrm{ns}^{-1}$.

III. THERMODYNAMIC PROPERTIES

Liquid simulation cells are quenched from 6000 K down to 10 K at zero pressure with variable cooling rates R ranging from 0.5 to 150 K/ps. The cell prepared with $R = 0.5$ K/ps is almost identical to the perfectly relaxed reference cell (see Sec. II). The corresponding fictive temperatures[33,34] of the liquid-glass transitions are obtained by the intersection points of the mutually extrapolated enthalpy and volume curves from the liquid and glassy sides, respectively, and are found in the interval, 463–618 K. The onset of the liquid-glass transition occurs at ≈715 K for cooling down with any of the investigated rates. Figures 1 and 2 show the resulting enthalpies and volumes per atom, respectively, as determined at 10 K directly after quenching.

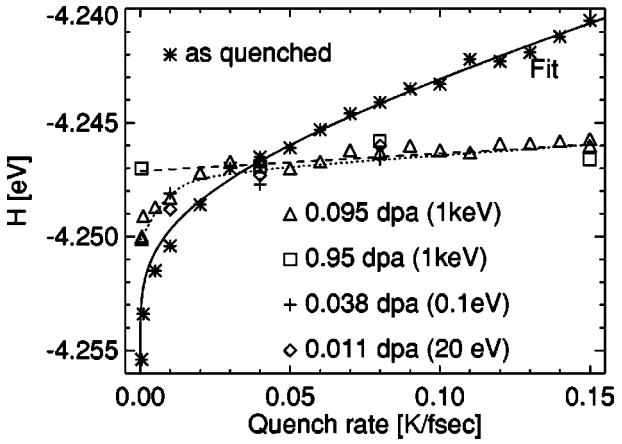

FIG. 1. Enthalpies of a-CuTi as a function of quench rate before and after ion bombardment with different energies and doses ($T=10$ K). For high enough doses, a universal steady state is reached (dashed line), which is independent of the thermal history of the glass, as well as the ion energy. The solid line is a fit to the enthalpy directly after quenching, assuming a logarithmic dependence on the cooling rate; the other lines are merely guides to the eye.

Both curves can be reasonably well fitted by assuming a logarithmic dependence on the rate R,

$$\ln\left(\frac{R}{R_0}\right) = -\frac{C}{X - X_0}, \tag{2}$$

where X denotes either the enthalpy or the volume, X_0 and R_0 correspond to some arbitrary reference rate, and C is a fitting constant. This is based on the observation, that below the glass transition both, enthalpy and volume, usually depend linearly on the temperature with identical slopes and are merely shifted in dependence of the thermal history. This shift is generally proportional to the shift of the fictive temperature T_f, which depends logarithmically on the cooling rate[12,35]

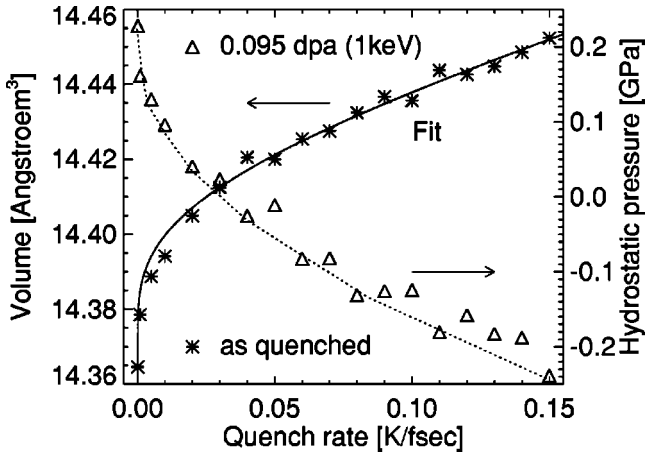

FIG. 2. Dependence of the average atomic volume on the quench rate and buildup of hydrostatic pressure after bombardment with 1 keV recoils. The solid line is a fit, assuming a logarithmic dependence of the volume on the cooling rate, the dotted line is just a guide to the eye.

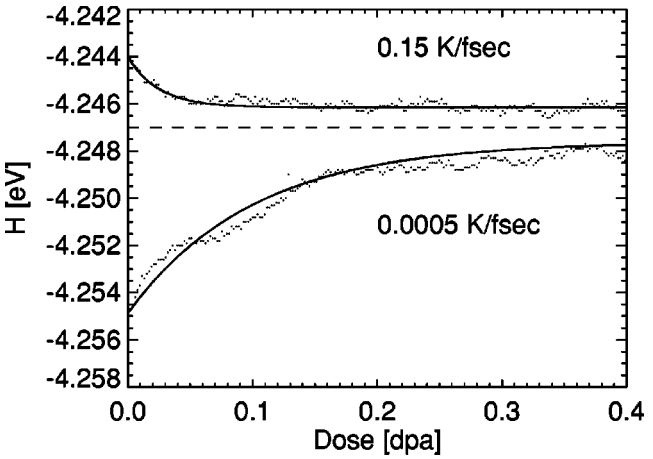

FIG. 3. During bombardment with 1 keV recoils, the enthalpies of differently prepared systems converge exponentially toward a steady state, which is greatly independent of the thermal history. The solid lines are exponential fits.

$$R = R_0\, \mathrm{e}^{-E_a/(kT_f)}, \tag{3}$$

with constants R_0 and E_a.

In the following we first focus on the modification of the enthalpy levels due to ion bombardment with 1 keV recoils at 10 K, as shown in Fig. 1. As a main result, relaxation is observed in systems that were initially quenched with $R \approx 0.04$ K/fs or higher, while increasing enthalpies occur in the case of more relaxed samples. For high enough doses, a steady state is observed ($H \approx -4.246$ eV, dashed line in Fig. 1), which is reached only by systems quenched with $R \gtrsim 0.02$ K/fs when loaded with 0.095 dpa. More relaxed configurations require higher doses, which is shown in Figs. 1 and 3. It is interesting to note, that an initial quenching rate of 0.04 K/fs exactly reproduces the enthalpy of the steady state, which does not reveal any further modification under recoil bombardment. A detailed analysis of the simulation cell during 1 keV recoils clearly shows the presence of melted regions in the sense of thermal spikes, which are not significantly expected[36] for the lower recoil energies[9] as investigated in Fig. 1. Nevertheless, even a sufficiently high amount of 20 eV recoils is capable of driving the system exactly towards the same steady state enthalpy, which therefore seems to be universally determined only by the sample temperature. It is generally found, that the enthalpy converges toward steady state with a decaying exponential as a function of dose Φ (see Fig. 3), i.e., $H = H_0 + H_1 \exp(-\Phi/\Phi_0)$, where Φ_0 is independent of the recoil energy, when measured in displacements per atom, and depends solely on the initial relaxation state of the system. In fact, we carried out comparable simulations at 300 K (not shown here) and obtained almost identical enthalpy and steady-state curves, just shifted toward more positive values, as expected. This indicates the universal nature of the observed phenomena.

The simulations above were performed at constant volume, which results in the buildup of compressive and tensile pressures once the steady state has been reached; that is, an

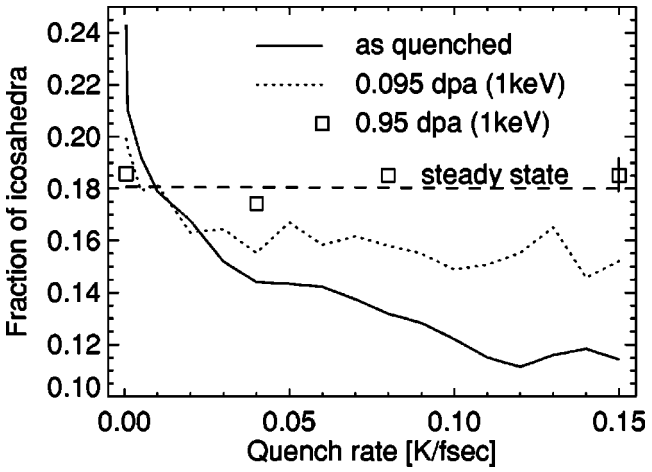

FIG. 4. Fraction of icosahedral-type of nearest-neighbor shells, as determined from the structural order parameter. The solid line is an interpolation to the *as quenched* samples, the dotted line after bombardment with 0.095 dpa (1 keV).

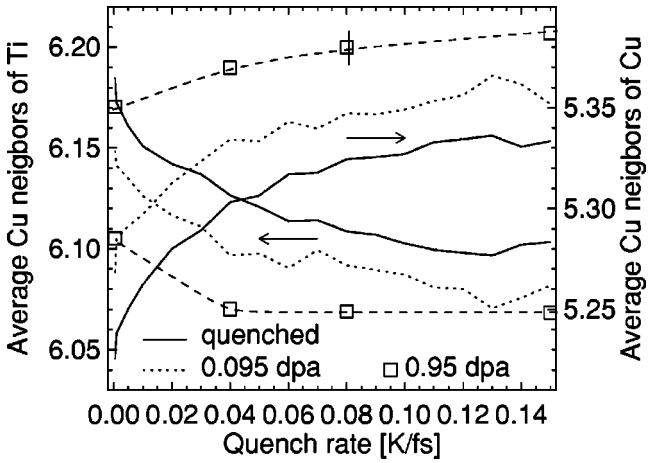

FIG. 5. Recoil-induced modifications of the composition of the nearest-neighbor shells in dependence of the initial quenching rate, with Cu and Ti as a central atom, respectively (recoil energy: 1 keV).

initially more relaxed sample expands and less relaxed sample contracts, respectively (Fig. 2). However, the stresses are so tiny, that they do not influence the relaxation behavior and steady state. This was confirmed by constant pressure simulation runs for samples with $R=5\times10^{-4}$ and 0.15 K/fs; these additional results are also incorporated in Fig. 1 in complete agreement with the constant volume data.

The glass transition temperature is determined for all samples before and after recoil bombardment by traversing a temperature ramp with the rate, 0.001 K/fs. It is found that it lies within the range $T_g \approx (736\pm10)$ K, where less relaxed matter tends to lower values, as expected.

IV. STRUCTURAL AND COMPOSITIONAL SHORT-RANGE ORDER

The modifications of the enthalpies and volumes of the simulation cells in dependence of the quench rates and ion treatments must be the effect of changes in the atomic-level structures of the amorphous solids, i.e., the structural and compositional short- and medium-range orders. For a more thorough investigation, the structural order parameter P_{st} is employed with respect to fcc, hcp, bcc, and ico short-range ordering. It is found, that none of the investigated CuTi samples shows any significant amount of a crystal-type SRO; portions are fluctuating around $\approx$0.5%. This again confirms their amorphous nature. However, the structural analysis yields a significant contribution of a local icosahedral type of ordering, which is energetically favorable, as shown in Fig. 4. The relevance of local ico configurations for glass formation has indeed been identified in simulations[28,30,37] and experimental[38] studies, as predicted before.[39,40]

Successive recoil bombardments change the structural environment in a-CuTi, by decreasing ($R<0.01$ K/fs) or increasing ($R>0.01$ K/fs) ico order, respectively, until a steady state is reached, which is greatly independent of the thermal history (Fig. 4). In comparison to the system enthalpies (Fig. 1), the steady state is reached at significantly higher doses (up to 0.95 dpa), which was simulated only for four representative samples due to the high CPU demand.

In addition, recoil bombardment has the effect of changing the local composition within the nearest-neighbor shells, which is shown in Fig. 5 for Cu neighbors around a Ti and Cu central atom, respectively. This effect has some similarity to ion-beam mixing (see Ref. 41 for a simulation). We also expect the occurrence of a steady state, which is, however, not fully observed for any of the simulations in Fig. 5. Even at the highest doses (0.95 dpa) only the samples quenched at $R\gtrsim0.04$ K/fs show some sign of saturation. As mixing occurs significantly slower than the enthalpy changes, this indicates, that compositional SRO has only a minor influence on the enthalpy H in a–CuTi. In fact, a rather weak influence of antisite defects on the enthalpy during amorphization of crystalline CuTi has been reported before.[17]

V. MECHANICAL PROPERTIES

The irradiation-induced energetic and structural modifications of the amorphous matrix in Sec. III and IV may seem small, they induce, however, severe effects on macroscopic properties. Figure 6 shows the dependence of the Young's moduli E on the quenching rates—before and after bombardment with 0.095 dpa recoils at 1 keV. The *as-quenched* samples reveal a strong decrease of almost a factor 3, from $\approx$66 GPa down to 27 GPa, when increasing the quench rates from 5.0×10^{-4} to 0.15 K/fs, respectively. When the samples are bombarded with energetic recoils, the elastic properties again reflect a steady state into which the system is driven by the forcing of irradiation, similar to the enthalpies (Fig. 1) and structures (Fig. 4). The steady-state value of $E\approx67$ GPa, which is reached at high enough doses, corresponds to a sample, which has been thermally quenched at $R\approx0.02$ K/fs. Similarly big effects have been reported experimentally for thermal treatment.[42]

Stress-strain curves are the other mechanical property investigated within the current scope. Figure 7 presents the

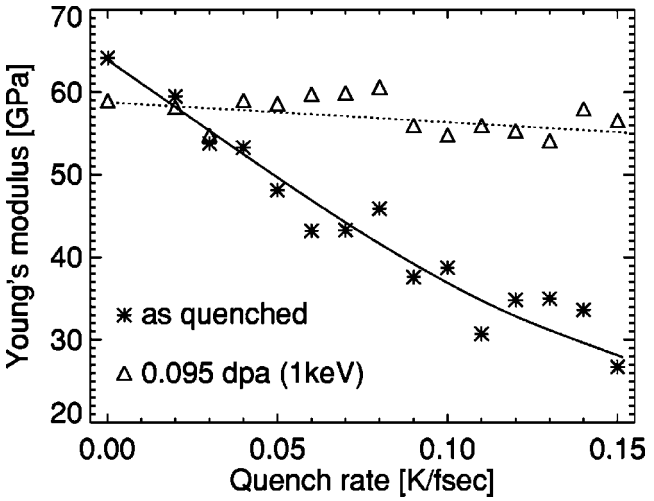

FIG. 6. Modifications of the elastic moduli of a-CuTi by recoil bombardments: Independent of the thermal history, a steady state elastic modulus is reached at high enough doses. The lines are guides to the eye.

result for three different quenching rates, where the as-quenched state is (a) more, (b) equal, and (c) less relaxed than the final radiation-induced steady state. It is observed that as the cell is more relaxed, the maximum strength increases, which is in agreement with experimental observations.[43,44] Again, in the steady state the stress-strain curves become greatly independent of the thermal history and behave similar to the sample quenched at ≈ 0.04 K/fs. In this context it is important to emphasize, that the presently employed potential does not include a covalent-bonding contribution or angular forces, and therefore overestimates the fluidity and ductility in comparison to experiments.

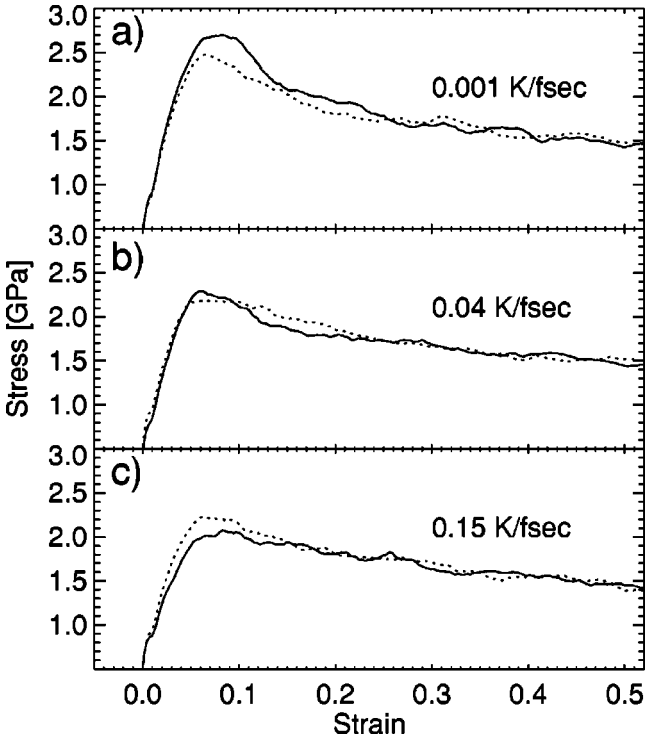

FIG. 7. Stress-strain curves of a-CuTi before (solid line) and after (dotted line) bombardment with 1 keV recoils (0.095 dpa), in dependence of the initial quench rate.

VI. DISCUSSION OF THE STEADY STATE

The investigations of key materials properties (Sec. III–V clearly indicate that ion irradiation drives different metallic amorphous phases toward *the same* steady-state amorphous phase. In fact, equivalent thermal and mechanical properties are clear manifestations of identical structural and compositional properties occurring on the atomic scale, i.e., the short-range order (Sec. IV) and beyond. This is a special feature of metallic glasses, which is, e.g., not observed in covalent network glasses.[45] In the following we therefore discuss the underlying atomic-scale kinetics.

It is tempting to utilize a thermal-spike-related model as a first simple picture. That is, metallic glasses are generally densely packed, so that nuclear stopping can elevate the local temperature within the cascade above the corresponding glass temperature at high enough recoil energies. As in the liquid state, the memory kernel[46] of the thermal history is lost, subsequent cooling down defines a newly quenched-in glassy state, which appears macroscopically, once the sample has been fully covered with thermal spikes.

Although the above picture is appealing because of its simplicity, it has some severe shortcomings. Particularly, it cannot explain why identical steady states are reached for any investigated recoil energy, even for energies as low as 20 eV, where melting within a thermal spike has been excluded.[9] This indicates, that a more generalized picture is desirable, which we base in the following on point-defect-like entities ("point defects") in the amorphous matrix.

We first note, that interstitials, vacancies, Frenkel pairs, as well as displacements can be defined in an amorphous matrix in analogy to their crystalline counterparts.[9] Similar to crystals, displacements introduce structural and compositional disorder. However, as lattice sites are not conserved, the kinetics of concurrent defects is found to be fundamentally different. In contrast to freely migrating defects[4] in crystalline systems, which can cover long distances by a diffusion process, point defects in metallic amorphous systems are easily delocalized and absorbed by the surrounding glassy matrix. This is achieved by viscous relaxation involving several neighboring shells of the defects, as shown in our earlier work.[9] Under external or thermodynamic forcing, this effect can be described as radiation-induced viscosity, $\Pi = \eta \cdot \dot{\Phi}$, while regular diffusion processes do not play any significant role at ambient temperatures. Thus, within the current context, radiation-induced viscous relaxation counteracts radiation-induced structural disordering. In fact, we have shown[9] that point defects always dominate the relaxation kinetics, as they affect significantly larger volumes than do thermal spikes. This is also in accord with our present finding that equivalent structural changes are obtained for different recoil energies when doses are normalized to the defect generation (i.e., measured in displacement per atom, Secs. III–V).

In the following, therefore, we present a more generalized picture based on the concept of competing dynamics, using an appropriate set of order parameters b_μ to characterize small deviations from a stabilized amorphous reference state b_μ^0. Recoil bombardments change the order parameters in a double way: They relax them by an appropriate viscosity Π_μ and contrarily drive them out of equilibrium with rates, β_μ. Using irreversible thermodynamics,[33,34] this is described by

$$\frac{\partial b_\mu}{\partial \phi} = -\Pi_\mu^{-1}\frac{\delta G}{\delta b_\mu} + \beta_\mu, \tag{4}$$

where G is an appropriate free enthalpy functional. For small deviations, $b_\mu - b_\mu^0$, from the reference state, $\delta G/\delta b_\mu$ is taylored as $\approx C(b_\mu - b_\mu^0)$, with an appropriate constant C. It is readily seen, that b_μ converges exponentially toward b_μ^{st}, given by

$$b_\mu^{\mathrm{st}} = b_\mu^0 + \Pi_\mu(\beta_\mu/C). \tag{5}$$

This atomic-scale picture, therefore, clearly explains the convergence of structural and compositional order toward a universal steady state in which thermal relaxation and external disturbance are balanced, as observed in Secs. III–VI.

VII. CONCLUSIONS AND OUTLOOK

Ion-beam bombardment drives differently structured amorphous phases toward a universal steady-state phase, which is independent of the thermal history. This is reflected by key physical properties, as demonstrated for thermodynamic, structural, and mechanical aspects. The final steady state is defined by a competition between radiation-induced disordering and viscous relaxation toward local equilibrium. From a practical point of view, the present studies suggest amorphous metallic alloys as an ideal engineering material in a radiation environment or deep space, especially as composites,[47] where radiation-induced viscous flow[9] should be greatly inhibited. Vice versa, ion-beam bombardment can be the method of choice to tune surface properties (such as hardness or wear resistance) of bulk metallic glasses, which is highly relevant for engineering applications.

ACKNOWLEDGMENTS

The author is indebted to Professor Dr. K. Samwer, Universität Göttingen, Germany and Professor R. S. Averback, University of Illinois at Urbana-Champaign, for valuable discussions and support. Funding by the Deutsche Forschungsgemeinschaft (DFG), SFB 602, TP B3, as well as a grant of computer time by the Gesellschaft für wisschenschaftliche Datenverarbeitung Göttingen (GWDG), Germany are gratefully acknowledged.

*Electronic address: smayr@uni-goettingen.de

[1] F. Seitz and J. S. Koehler, Solid State Phys. **2**, 305 (1956).
[2] R. S. Averback and T. D. de la Rubia, Solid State Phys. **51**, 281 (1998).
[3] M. B. H. Breese, *MRS Bulletin, Volume 25(2)* (Materials Research Society, Warrendale, 2000).
[4] L. E. Rehn, P. R. Okamoto, and R. S. Averback, Phys. Rev. B **30**, 3073 (1984).
[5] G. Martin and P. Bellon, Solid State Phys. **50**, 189 (1996).
[6] W. L. Johnson, MRS Bull. **24**(10), 42 (1999).
[7] S. Klaumünzer and G. Schumacher, Phys. Rev. Lett. **51**, 1987 (1983).
[8] P. Jung, J. Appl. Phys. **86**, 4876 (1999).
[9] S. G. Mayr, Y. Ashkenazy, K. Albe, and R. S. Averback, Phys. Rev. Lett. **90**, 055505 (2003).
[10] S. G. Mayr and R. S. Averback, Phys. Rev. Lett. **87**, 196106 (2001).
[11] S. G. Mayr and R. S. Averback, Phys. Rev. B **68**, 214105 (2003).
[12] J. Zarzycki, *Glasses and the Vitreous State* (Cambridge University Press, Cambridge, 1982).
[13] T. Mattila, R. M. Nieminen, and M. Dzugutov, Nucl. Instrum. Methods Phys. Res. B **102**, 119 (1995).
[14] M. P. Allen and D. J. Tildesley, *Computer Simulation of Liquids* (Oxford Science Publications, Oxford, 1987).
[15] M. J. Sabochick and N. Q. Lam, Phys. Rev. B **43**, 5243 (1991).
[16] S. G. Mayr and R. S. Averback, Phys. Rev. B **68**, 075419 (2003).
[17] N. Q. Lam, P. R. Okamoto, and M. Li, J. Nucl. Mater. **251**, 89 (1997).
[18] H. Teichler, J. Non-Cryst. Solids **312**, 533 (2002).
[19] Based on PARCAS (Ref. 22).
[20] M. S. Daw and M. I. Baskes, Phys. Rev. B **29**, 6443 (1984).
[21] J. F. Ziegler, J. P. Biersack, and U. Littmark, *The Stopping and Range of Ions in Matter* (Pergamon Press, New York, 1985).
[22] K. Nordlund and R. S. Averback, Phys. Rev. B **56**, 2421 (1997).
[23] H. J. C. Berendsen, J. P. M. Postma, W. F. van Gusteren, A. DiNola, and J. R. Haak, J. Chem. Phys. **81**, 3684 (1984).
[24] This is empirically achieved by monitoring the shock wave propagation for variable damping constants, resulting in $\tau \approx 50$ fsec for the present system (as described before—see, e.g., Ref. 48).
[25] SRIM 2003 computer code (Ref. 21).
[26] The situation is slightly different in the case of covalent network glasses, where strong pressure dependences are found (Ref. 45).
[27] G. Kinchin and R. Pease, Rep. Prog. Phys. **18**, 1 (1955).
[28] P. J. Steinhardt, D. R. Nelson, and M. Ronchetti, Phys. Rev. B **28**, 784 (1982).
[29] J. D. Honeycutt and H. C. Andersen, J. Phys. Chem. **91**, 4950 (1987).
[30] H. Jonsson and H. C. Andersen, Phys. Rev. Lett. **60**, 2295 (1988).
[31] H. Zhu, R. S. Averback, and M. Nastasi, Philos. Mag. A **71**, 735 (1995).
[32] With $\tau = 1$ psec, which prevents the occurrence of shockwaves, which can plastically deform the cell.
[33] I. Prigogine and R. Defay, *Chemische Thermodynamik* (VEB Deutscher Verlag für Grundstoffindustrie, Leipzig, 1962).
[34] I. Prigogine, *Thermodynamics of Irreversible Processes* (Interscience Publishers, Wiley, New York, 1967).
[35] H. Scholze, in *Reactivity of Solids*, edited by J. S. Anderson,

M. W. Roberts, and F. S. Stone (Chapman and Hall, London, 1972), p. 160.

[36] For recoil energies as low as 20 eV the lifetime of excitations is less than ≈5 lattice vibrations (Ref. 9), which is far from achieving local thermal equilibrium in the sense of the thermal spike concept.

[37] M. Guerdane and H. Teichler, Phys. Rev. B **65**, 014203 (2001).

[38] W. K. Luo, H. W. Sheng, F. M. Alamgir, J. M. Bai, J. H. He, and E. Ma, Phys. Rev. Lett. **92**, 145502 (2004).

[39] F. C. Frank and J. Kasper, Acta Crystallogr. **11**, 184 (1958).

[40] D. R. Nelson and F. Spaepen, Solid State Phys. **42**, 1 (1989).

[41] H. Gades and H. M. Urbassek, Phys. Rev. B **51**, 14559 (1995).

[42] H. S. Chen, J. Appl. Phys. **49**, 3289 (1978).

[43] H. Kato, Y. Kawamura, A. Inoue, and H. S. Chen, Appl. Phys. Lett. **73**, 3665 (1998).

[44] J. Lu, G. Ravichandran, and W. L. Johnson, Acta Mater. **51**, 3429 (2003).

[45] S. G. Mayr and R. S. Averback, Phys. Rev. B **71**, 134102 (2005).

[46] A. B. Mutiara and H. Teichler, Phys. Rev. E **64**, 046133 (2001).

[47] R. D. Conner, R. B. Dandliker, and W. L. Johnson, Acta Mater. **46**, 6089 (1998).

[48] K. Nordlund and R. S. Averback, Phys. Rev. B **59**, 20 (1999).